

# Semisolid extrusion molding of Mg-9%Al-1%Zn alloys

F. CZERWINSKI

*Development Engineering, Husky Injection Molding Systems Ltd., Bolton, Ontario, L7E 5S5, Canada*

A novel technique in manufacturing net-shape components of magnesium alloys, which combines semisolid processing, extrusion and injection molding, is outlined. For an Mg-9%Al-1%Zn composition, the high-temperature transformations and factors controlling solidification microstructures, are analyzed. © 2004 Kluwer Academic Publishers

## 1. Introduction

Extrusion is the plastic deformation process by which a metal is forced to flow by compression through the die orifice of a smaller cross-sectional area than that of the original billet. Since the material is subjected to compressive forces only, the extrusion is an excellent method for breaking down the cast structure of the billet with little or no cracking [1]. Most metals are extruded hot when the billet is preheated to facilitate plastic deformation, but room temperature (cold) extrusion is also exercised. So far, conventional extrusion applications do not utilize preheating materials above the solidus temperature to enter the semisolid range.

The advantages of processing metallic alloys in a semisolid state are attributed to the globular solid particles which control their thixotropic properties at high temperatures and reduce the content of dendritic forms after subsequent solidification [2]. It is well established that the benefits associated with semisolid processing, such as low shrinkage porosity, high tolerances and energy savings, are more evident at high solid fractions. Moreover, the ability to cast at higher solid fractions is of interest in improving billet stability and minimizing material loss during handling.

Of all semisolid technologies, injection molding provides the largest flexibility in terms of the processed solid contents [3]. This feature is attributed to the fact that injection molding combines the slurry making and component forming operations into one step, and the slurry is accumulated in a direct vicinity of the mold gate. So far, these potentials are not explored and commercial applications are limited to liquid-rich slurries, which, for thin-wall sections, may contain solid volumes as low as 5–10%. As the major obstacle preventing using high solid contents, the premature alloy's freezing and incomplete filling the mold cavity, is reported [4]. It was, therefore, anticipated that a drastic increase in solid content, especially above 60%, would transform the flow through the machine nozzle, runners, and mold gate into the extrusion, thus activating interaction between solid particles within the slurry which would facilitate the mold filling. The verification of such a hypothesis was the objective of this study.

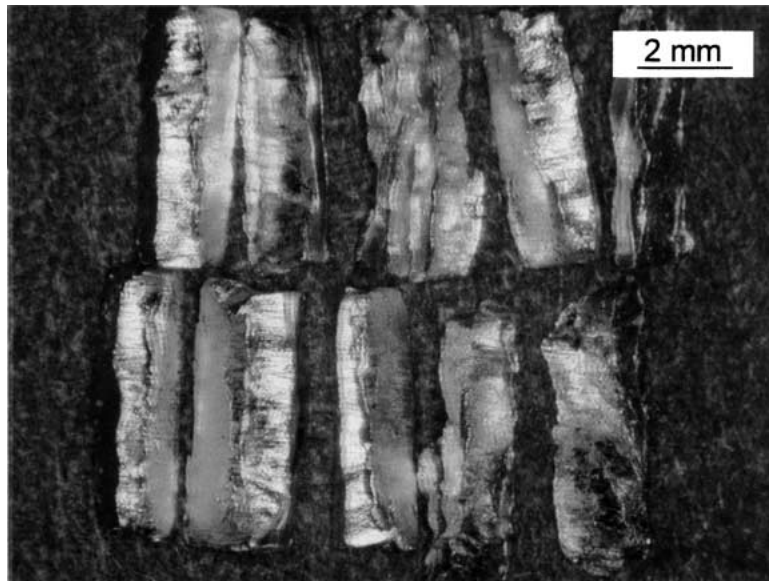
## 2. Experimental details

AZ91D magnesium alloy, used in the present study, had a nominal composition of 8.5% Al, 0.75% Zn, 0.3% Mn, 0.01% Si, 0.01% Cu, 0.001% Ni, 0.001% Fe and an Mg-balance. An as-cast ingot was mechanically converted into small chips and processed using a Husky TXM500-M70 prototype system with a clamp force of 500 tons and a 2 m long barrel with a diameter of 70 mm. The component manufactured represented the complex shape with a diameter of 190 mm and a total weight, including sprue and runners, of 582 g [3]. The mold was preheated to 200°C and the slurry was injected at a screw velocity in the range of 0.7–2.8 m/s. For the gate opening of 221.5 mm<sup>2</sup> it converts to the alloy's velocity at the mold's gate between 12.2 and 48.6 m/s. In order to examine the role of flow through the gate, the alloy was also injected (purged) into the partly open mold at significantly lower flow velocity at the mold gate. The typical cycle time was approximately 25 s, which corresponds to an average residency time of the alloy within the machine barrel of the order of 100 s. In some cases, the cycle time was deliberately extended up to 4 times. Metallographic samples of the molded alloy were prepared by grinding with progressively finer SiC paper, mechanical polishing with 1 μm diamond paste and colloidal alumina, followed by etching in a 1% solution of nitric acid in ethanol. Stereological analysis was conducted using optical microscopy, equipped with a quantitative image analyzer.

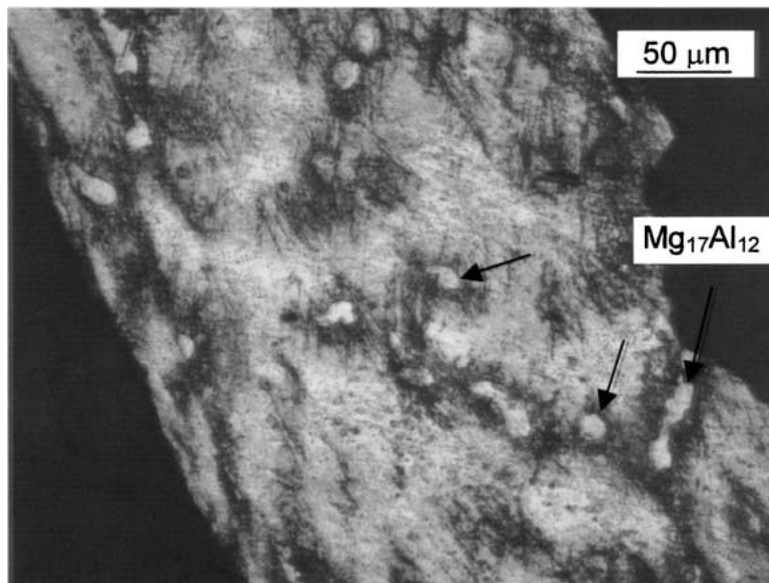
## 3. Results

### 3.1. Structural transformations of the alloy during processing

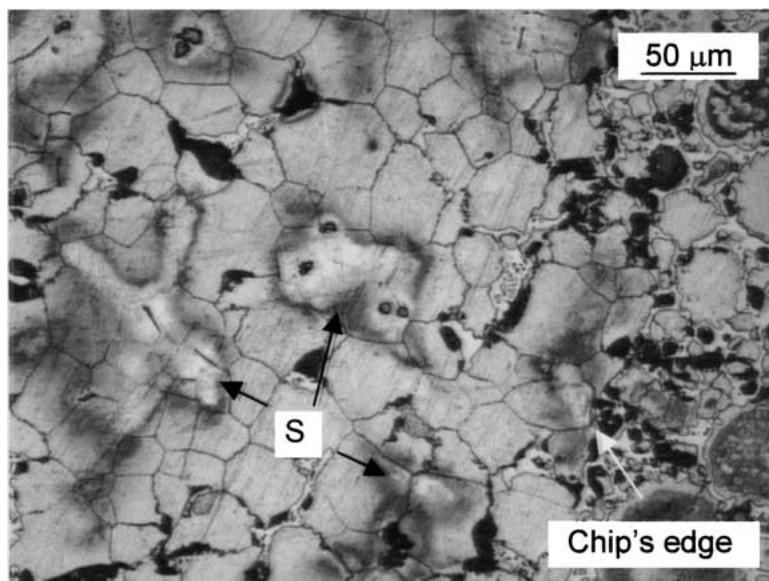
Morphologies of an as-chipped alloy are shown in Fig. 1a. According to size determination by the screen method ASTM E-276-68, the predominant fraction of chips was retained on sieves with openings within the range 0.6–2 mm, and 75% of them did not pass through the 1.4 mm sieve. As a result of interaction with the chipping tool, the alloy experienced a cold work. The chips' deformation is inhomogeneous with



(a)



(b)



(c)

*Figure 1* The initial state and thermal decomposition of Mg-9%Al-1%Zn feedstock, used during experiments: (a) as-received chips, (b) chip's cross-section with cold-work features and (c) early stage of chip's melting, showing disintegration of equiaxed network of recrystallized grains; the chemical segregation contour of former dendritic features, consumed by equiaxed grains is marked as "s".

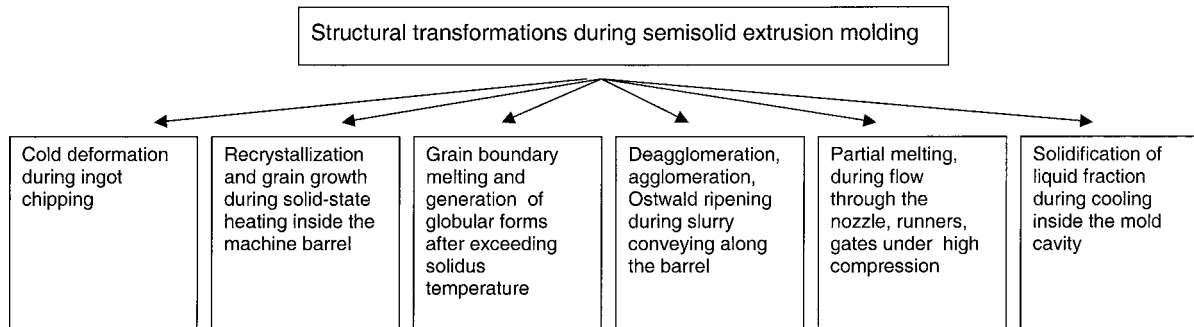


Figure 2 The schematic diagrams of structural transformations of a magnesium alloy during various stages of the semisolid extrusion molding.

an increased strain in an immediate location of the second phase particles (Fig. 1b). As proven by chips melting outside the molding system, dendritic structure disintegrated completely by the solid-state reaction (Fig. 1c). During heating inside the machine barrel, the structure recrystallized by nucleation and the growth of equiaxed grains. The second phase, intermetallic compound  $Mg_{17}Al_{12}$ , was distributed mainly along grain boundaries. In addition, grain boundaries were enriched in the solute element Al. After exceeding the solidus temperature, the melting started at grain boundaries leading first to the generation of equiaxed, then globular solid particles, surrounded by the liquid metal (Fig. 1c). The summary of major structural transformations during semisolid extrusion molding is shown in Fig. 2. Thus, during further conveying of the slurry along the barrel, the globular structures of the unmelted phase experienced breakdown and agglomeration due to the combined effect of external heat and strain. As a result of diffusion, the solid phase was also subjected to coalescence and Ostwald ripening, as discussed in detail previously [5]. After melting of the grain boundary network, the semisolid slurry, with globular solid particles, was essentially ready for the component-forming step, i.e. the injection into a mold cavity.

### 3.2. Solidification microstructures

The microstructure, typical for ultra-high solids is comprised predominantly of unmelted particles of  $\alpha$ -Mg, surrounded by a solidification product of the former liquid phase. As seen in Fig. 3a, the particle's shape is near globular, but with increasing solid fraction it shows a tendency to be more constrained geometrically, exhibiting shape accommodation. The former liquid covers the grain boundary network with small pools accumulated at triple junctions. There were also randomly distributed larger islands of the liquid; however, they were generally smaller than the solid particle. The portion of the former liquid which was entrapped within solid particles showed high dispersion. Thus, instead of single island morphologies, frequent for medium and lower solid fractions [6], there were numerous randomly distributed precipitates of smaller size and globular shape. It is likely that some of them were formed by solid-state precipitation from the supersaturated solid solution than by solidification of the Al-rich liquid.

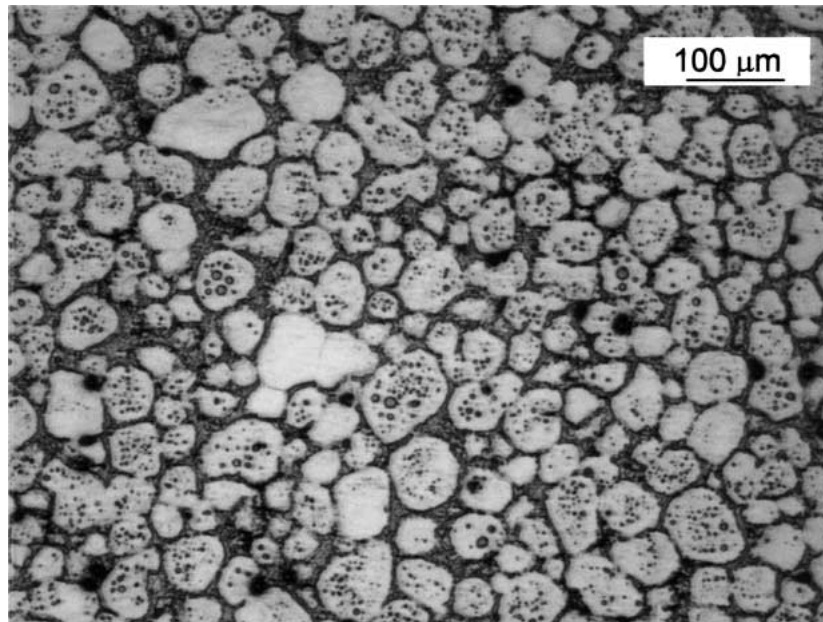
### 3.3. Microstructural feedback towards the high-temperature stage

The detailed examination of room-temperature microstructures provided important information regarding phenomena which take place at high temperatures. A strong influence of alloy injection velocity on the solidification morphologies was discovered. An example in Fig. 3b represents the structure formed from the slurry with the same initial solid content as that in Fig. 3a. The major processing difference was approximately a 100% increase in the mold gate opening and component wall thickness. The structure in Fig. 3b solidified in 4 mm-thick sections. Thus, reduction in injection velocity, combined with increased component wall thickness, led to the transition from globular particles surrounded by freshly solidified matrix to equiaxed grains. Some occasional islands of the former liquid were distributed at triple junctions. There is no substantial difference in the volume fraction and dispersion degree of precipitates within grain interiors, as compared to those present within globular solid particles (Fig. 3a).

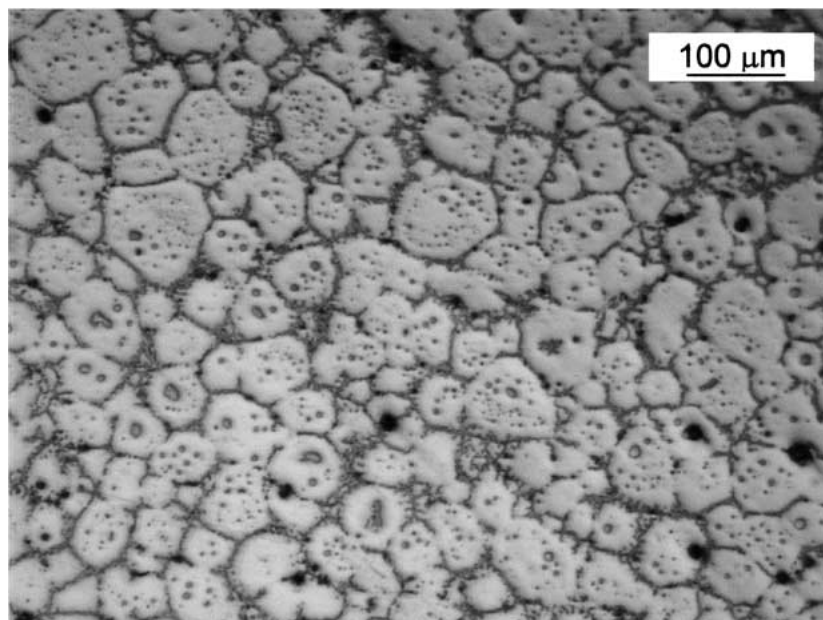
The quantitative description of the influence of the injection rate on the molded structure is shown in Fig. 4. The first finding is that for a given initial solid content within the slurry, the higher injection velocity led to an increased liquid content inside the part. In addition, the injection velocity affected the homogeneity of solid particle distribution, particularly across the part thickness. While for the gate velocity of 12.2 m/s the solid fraction across the part thickness of 2 mm remained constant, the velocity of 48.6 m/s caused an increase in the liquid fraction towards the component outer surface. For 12.2–48.6 m/s range of injection velocities, there was an increase in average liquid content from 15 to 25%. It seems that there was not close relationship between the solid content or its distribution and a size of the unmelted phase, which is characterized by the histogram in the insert of Fig. 4. The solid particle size was, however, strongly affected by the alloy's residency time inside the machine barrel. An increase of average cycle time by four times, resulting in a total residency time of 400 s increased the average particle size from 33  $\mu\text{m}$  to 60  $\mu\text{m}$ .

## 4. Discussion of results

The key requirement of semisolid processing is the thixotropic slurry with non-dendritic morphologies of



(a)



(b)

*Figure 3* The microstructure of AZ91D alloy obtained from the slurry with the same solid fraction: (a) globular structure, injection velocity of 48.6 m/s, wall thickness of 2 mm and (b) equiaxed structure, injection velocity of 5 m/s, wall thickness of 4 mm.

the unmelted phase. Our finding [6, 7] that the cold work, imposed on chips during their manufacturing, is a driving force for the generation of globular forms by the mechanism of recrystallization and grain boundary disintegration implies that such a slurry is formed at the very beginning of melting (Fig. 1b and c). Since all benefits are associated with the unmelted solid phase it would appear that the liquid content should be kept as low as possible. However, a certain liquid content is required to ensure processibility, defined as the macroscopically homogeneous and damage free flow. This minimum depends on the alloy type, and for the aluminum alloy A 2014, deformed in an unconstrained compression, it was as low as 20% [8]. In the case of this study, the minimum value was even lower (Fig. 4).

It is generally accepted that, at ultra-high solid contents, the alloy represents a deformable, semi-cohesive granular solid, saturated with liquid. When subjected to external strain, the alloy will respond by the disagglomeration of partially bonded grains. It is highly possible that, due to the shear imposed by the screw and relatively short rest time, there is no bond between the solid particles accumulated directly before injection. Analyses of as-solidified structures (Figs 3a and 4) and machine operating parameters suggest that phenomena of solid/solid interaction within the slurry with ultra high solid contents are significantly more intense than those described for low and medium solid contents. During semisolid injection molding, the mold filling time is the key factor which controls the entire process [3]. If the material experiences solidification (freezing), it reduces

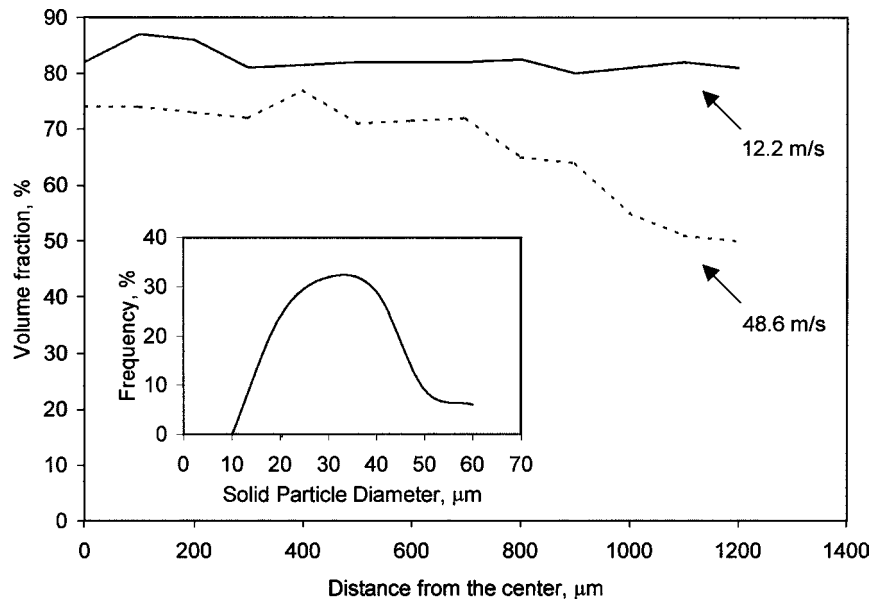


Figure 4 The inhomogeneity in the distribution of solid particles within the component, extrusion molded in a semisolid state. The inset shows a typical histogram of solid-size distribution at middle-wall thickness.

the cross section of the flow channel and increases the effective filling time. It is suspected that the interparticle interference, at the stage of injection, facilitates the mold filling process. This hypothesis is supported not only by the complete mold filling, but also by the fact that the mold filling time was approximately 0.025 s, which is of the same order of magnitude as that measured for low solid contents.

The characteristic feature of microstructures produced by semisolid extrusion molding is the small size of the unmelted phase (Fig. 4, inset). This size being of 34  $\mu\text{m}$ , is very similar to the grain size within the recrystallized chip and was believed to be preserved by external shear causing disagglomeration [5, 9]. An increase in the cycle time to 100 s mainly affected the alloy's residency time in an absence of shear. It is natural that the system reduces its energy by particle growth, although mechanisms may differ from those described for low solid contents. At solid fractions above 0.5, coarsening behaviour can better be described by considering the migration of the liquid films separating the grains, than by considering diffusion fields around isolated solid grains, as in the Lifshitz, Slyozov and Wagner analysis [10]. Coarsening cannot be used exclusively to explain the formation of the equiaxed structure in Fig. 3b. Rather, the reduced gate velocity and longer solidification time, caused by thicker alloy section, provide a better answer. According to this mechanism, solidification of the liquid portion of the alloy takes place on pre-existing globular substrates as described earlier for large slurry volumes, which solidified inside the machine barrel [9].

The inhomogeneities in the solid phase distribution of as-solidified structures (Fig. 4) result from the flow characteristics during mold filling. The higher solid content in the part than within the runner should be interpreted as resulting from melting during slurry flow through the narrow gate channels. Similar findings were reported for experiments of the back extrusion of Sn-

Pb alloy with an effective liquid fraction of less than 0.30, where it was found that the liquid fraction was a function of the extrusion ratio increasing as the wall thickness decreased [11]. Another possibility of the selective flow where the liquid fraction is pushed through the solid skeleton seems to be diminished, from the microstructural analysis of samples taken along the alloy flow path. The relatively high flow velocity of the alloy during mold filling and specific gravity difference between solid and liquid causes phase segregation. For an injection velocity of 49.6 m/s, the liquid content close to the outer surface is about 20% higher than in the center (Fig. 4). Details of the inhomogeneous distribution of the solid phase within the part still requires explanation.

## 5. Conclusions

The elements of semisolid processing, extrusion and injection molding were successfully combined to manufacture net shape components of Mg-9%Al-1%Zn alloy starting from a slurry with high solid contents of the order of 70%. The resultant solidification microstructures ranged from globular forms surrounded by the former liquid matrix to exclusively equiaxed grains.

At high temperatures, the unmelted particles were susceptible to coarsening with increased residency time and the homogeneity in their distribution within the part was influenced by the injection velocity. It is believed that the phenomenon of solid particle interference during slurry flow under compressive forces facilitated filling the mold cavity.

## References

1. G. E. DIETER, "Mechanical Metallurgy" (McGraw-Hill, New York, 1976).
2. M. C. FLEMINGS, *Metall. Trans. A* **22** (1991) 957.
3. F. CZERWINSKI, *Adv. Mater. Proc.* **160/11** (2002) 31.

4. D. M. WALUKAS, R. E. VINING, S. E. LEBEAU, N. TANIGICHI and R. F. DECKER, *Advanced Semisolid Processing of Alloys and Composites*, edited by Y. Tsutsui, M. Kiuchi and K. Ichikawa, Tsukuba, Japan, 2002, p. 101.
5. F. CZERWINSKI, *Scripta Mater.* **48** (2003) 327.
6. F. CZERWINSKI, A. ZIELINSKA-LIPIEC, P. J. PINET and J. OVERBEEKE, *Acta Mater.* **49** (2001) 1225.
7. F. CZERWINSKI, *ibid.* **50** (2002) 3265.
8. E. TZIMAS and A. ZAVALIANGOS, *ibid.* **47** (1999) 517.
9. F. CZERWINSKI, *Metall. Mater. Trans. A* **33** (2002) 2963.
10. E. D. MANSON-WHITTON, I. C. STONE, J. R. JONES, P. S. GRANT and B. CANTOR, *Acta Mater.* **50** (2002) 2517.
11. T. BASNER, R. PEHLKE and A. SACHDEV, *Metall. Mater. Trans. A* **31** (2000) 57.

*Received 23 April  
and accepted 12 August 2003*